JSCEI Journal of Sustainable Civil Engineering Insights

Original Research Article

Analysis of Capacity and Ductility in Mortar-Filled Hollow Steel Frames with Variable Horizontal Bar Spacing

M. Saumi Rizaldi[a], Saffuan Wan Ahmad[b*], Kavitha P.E.[c], Rahimi A. Rahman[d,e]

[a] *Department of Civil Engineering, Universitas Muhammadiyah Aceh, Banda Aceh 23245, Indonesia*
[b] *Faculty of Civil Engineering, Universiti Malaysia Pahang Al-Sultan Abdullah, Kuantan 26600, Malaysia*
[c] *Department of Civil Engineering, Federal Institute of Science and Technology, Angamaly 683577, India*
[d] *Faculty of Civil Engineering, Universiti Malaysia Pahang Al-Sultan Abdullah, Kuantan 26600, Malaysia*
[e] *Faculty of Graduate Studies, Daffodil International University, Dhaka 1216, Bangladesh*

*Corresponding author: saffuan@umpsa.edu.my

Highlights:

- Experimental capacity was consistently lower than ETABS predictions, indicating that numerical modeling overestimates the real strength of mortar-filled perforated steel frames; a reduction factor of 0.5 is recommended for practical design.
- RBH Type 3 achieved the highest load capacity (3.872 tf) and good ductility (3.37), suggesting that closer horizontal bar spacing improves structural performance.
- All specimens demonstrated adequate ductility (2.24–4.61) under monotonic pushover loading, confirming the potential of mortar-filled hollow steel frames as a viable alternative to wood-based wall reinforcement systems.

Abstract: The use of wood in the construction industry results in forest degradation, which can negatively impact the natural environment. To reduce the use of wood, alternative materials are needed. Steel is one such alternative due to the wide availability of steel products on the market. The purpose of this study is to determine the capacity and ductility of frames used as wall reinforcement by employing perforated steel filled with mortar. This research involves a hollow steel frame filled with mortar and reinforced with welded joints, with variations in the spacing between horizontal bars. The study was conducted using Extended Three-dimensional Analysis of Building Systems (ETABS) application modeling and experimental laboratory tests. The results of the capacity and ductility from the test data are compared with the results from ETABS application modeling, allowing for adjustments when modeling real-world conditions. The plane frame of the test object, designed according to the plan, was subjected to a monotonic load (pushover) on the left side until the planned deflection was reached. The results indicate that the maximum load capacity in laboratory testing for each specimen variation is lower than that predicted by ETABS modeling. The maximum capacities for Hollow Steel Frame (RBH) Type 1, Type 2, and Type 3 specimens are 2,895tf, 2,721tf, and 3,872tf, respectively, while for the ETABS application, they are 4.8tf, 5.6tf, and 5.8tf, respectively. Therefore, a reduction factor of 0.5 from the ETABS modeling results is needed for the use of similar construction in the future. The ductility values for RBH Type 1, Type 2, and Type 3 specimens were 4.61, 2.24, and 3.37, respectively.

Keywords: Capacity, ductility, hollow steel, horizontal, plane frame

1. Introduction

One of the main raw materials needed for the construction of buildings and houses is wood. The continuous use of wood results in deforestation, leading to forest degradation and worsening the state of the surrounding environment [1]. To meet the public demand for sufficient raw materials for the construction of buildings and houses, alternative materials that can replace wood are needed.

Steel is one such material that has a fairly good ability to withstand tensile forces [2]. Hollow steel, a type of steel bar with a cavity in the middle, is commonly used in the construction industry. It can serve as the primary raw material for both structural and non-structural construction work. However, hollow steel has a weakness in that it is prone to buckling [3]. To mitigate this issue, hollow steel is often filled with mortar.

Mortar is a mixture of fine aggregate (sand), adhesive material, and water. The adhesive material can be clay, lime, or cement [4]. The quality of mortar can be determined by creating cube test specimens and testing them at 14, 21, and 28 days of age [5]. Mortar can function as filling material for the void in the hollow steel cavity, helping to prevent excessive buckling [6].

Received: 27 June 2024
Revised: 20 August 2025
Accepted: 08 December 2025
Published: 18 February 2026

In this research, three test pieces with different designs and shapes were studied. Each test specimen consisted of hollow steel connected using welding, with the cavity filled with mortar. Variations in the spacing between horizontal bars were introduced to study their impact on deflection reduction [7]. Horizontal rods are expected to reduce the deflection that occurs in the column due to horizontal forces. The different horizontal spacings tested were 1.25 m for RBH Type 1, 0.83 m for RBH Type 2, and 0.625 m for RBH Type 3. The hollow steel used had dimensions of 100/100, 50/100, 30/60, 20/40, and 20/20. The mortar materials included PCC cement, fine aggregate, water, and additives such as sika viscocrete-10 [8]. The manufacture of test specimens involved cutting the hollow steel as planned and filling the cavity with mortar. To ensure the desired quality of the mortar, 50 mm x 50 mm x 50 mm cube specimens were tested at 14, 21, and 28 days of age until the specified quality was achieved. The support used in this test was joint support [9].

This research hypothesizes that the more horizontal bars present, the load received by the column will be distributed across each bar, increasing the capacity and ductility of the plane frame. The purpose of this research is to determine the capacity and ductility of the hollow steel frame in resisting monotonic loads (pushover) with variations in horizontal rod spacing. Additionally, it aims to estimate the capacity of the plane frame using the Load and Resistance Factor Design (LRFD) approach to predict the ultimate force that can be carried by the plane frame, which is then compared with experimental results.

2. Materials and Methods

2.1. Planning of Plane Frame Structure

In the process of planning the plane frame structure, modeling was carried out using the ETABS application [2]. The structural modeling conducted in the ETABS application involved applying a monotonic load on the top left, which was also used during field testing [3]. The planned plane frame structure has three different types, differing in the spacing between the horizontal bars, and one type of plane frame serves as a control [10]. The images of the plane frame structure planning and their dimensions can be seen in Figure 1.

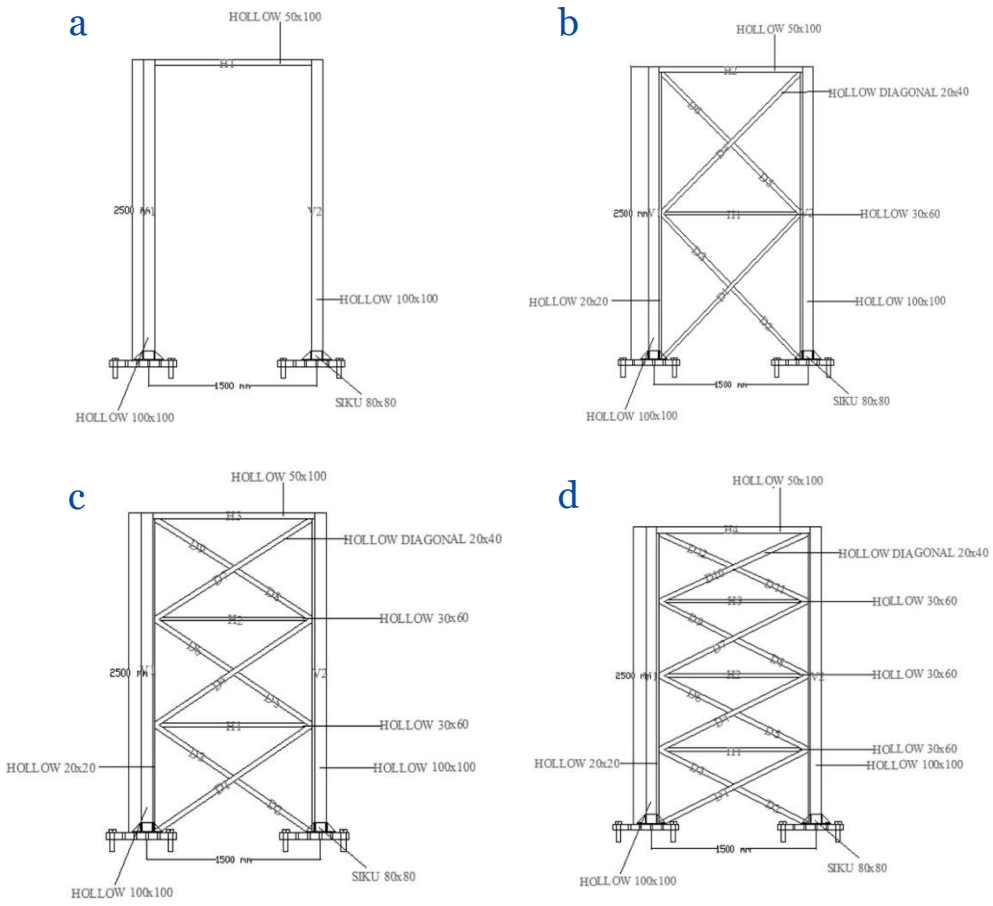

Figure 1. Structural Models of Plane Frames with Different RBH Types. (a) Modeling of control RHB; (b) modeling of RHB type 1; (c) modeling of RHB type 2; (d) modeling of RHB type 3.

2.2. Preparation Stages

The test objects in this study are formed as shown in Figures 1 and then connected using welding [11]. Details of the amount of hollow material used for the plane frame test objects are presented in Tables 1–4.

Table 1. Structure Bar Length RBH Control

Profile Size (mm)	Profile thickness (mm)	Element Length (mm)
100x100	2.5	5,000
50x100	1.7	1,500

Table 2. Structure Bar Length RBH Type1

Profile Size (mm)	Profile thickness (mm)	Element Length (mm)
100x100	2.5	5,000
20x20	1.7	10,000
30x60	1.7	1,500
50x100	2	1,500
20x40	1.7	15,620

Table 3. Structure Bar Length RBH Type2

Profile Size (mm)	Profile thickness (mm)	Element Length (mm)
100x100	2.5	5,000
20x20	1.7	5,000
30x60	17	3,000
50x100	2	1,500
20x40	1.7	20,592

Table 4. Structure Bar Length RBH Type3

Profile Size (mm)	Profile thickness (mm)	Element Length (mm)
100x100	2,5	5,000
20x20	1.7	5,000
30x60	1.7	4,500
50x100	2	1,500
20x40	1.7	26,000

The concrete mortar mix design in this study is based on the Indonesian National Standard (SNI) 7656-2012 [5]. The mortar was designed with K-400 quality, using a water-cement ratio (WCR) of 0.4 and a cement-to-sand ratio of 1:2. An admixture, sika discrete-10, was added at 1% of the cement weight to improve mortar density and ease the casting and filling process into the hollow steel cavities.

2.3. Stages of Implementation

The cutting of the hollow steel test pieces is carried out according to the planned sizes [13]. This process begins by marking the boundaries of the rod lengths as specified in Tables 1–4. The steel is then cut to the predetermined sizes.

During the casting process, the composition of the materials used follows the predetermined mix design plan [5]. Casting begins with checking the tools and materials to ensure they are in good condition. After verification, the casting process starts by putting sand, water, cement, and discrete-10 into the concrete mixer, mixing the materials until evenly blended for 3-5 minutes [6]. To control the strength of the mortar, test specimens are created for each plane frame, with three units per frame. These specimens are cubes measuring 50 mm x 50 mm x 50 mm.

The flow test is conducted when all the mortar materials are thoroughly mixed before being placed into the cube molds and hollow steel cavities [18]. The test begins by placing the well-mixed mortar into the flow mold, leveling it, lifting the mold, and then tamping it 25 times for 15 seconds. The final step is to measure the diameter of the mortar spread.

Once the mortar is prepared, it is injected into the hollow steel sections that have been cut to the planned sizes. The injection process is done manually until the hollow steel is filled. After filling all the cavities of the cut hollow steel bars with mortar, the next step is assembling the test objects

[11]. This assembly process involves welding the pieces together using a comprehensive welding method (Figure 2).

In this study, the mortar specimens are treated using the water-curing method. This involves immersing the mortar samples in water at a temperature of 20°C–30°C. The curing process lasts for 14 days, and if the desired quality is not achieved, it continues for 21 and 28 days. After curing, the mortar samples are allowed to stand for one day at room temperature before further testing.

This test ensures that the quality of the mortar used to fill the hollow steel meets the planned standards. Mortar compressive strength testing starts at 14 days. If the desired quality is not achieved, further tests are conducted at 21 and 28 days. The compressive strength tests are performed using a Compressive Strength Tester, brand Ton Industry No. 2551/90/1970, produced by Mannheim Germany, with a compressive capacity of 10 tons. This machine applies a constant load until the concrete fails. The testing procedure follows the Indonesian National Standard (SNI) 03-6825-2002 for testing the compressive strength of Portland cement mortar for civil works [14].

The field frame testing process uses a Linear Variable Displacement Transducer (LVDT) machine. This test involves placing the test object in a predetermined position and then applying a load on the top left of the test object, recording the resulting reactions. This test is conducted on each prepared specimen, following the mortar compressive strength testing. Before testing, the plane frame supports are welded to elbows bolted to the base plate to prevent shifting. The plane frame structure is then placed on the load frame tool, and the load is applied by placing a load cell on the upper left side of the test object. The load increases by 100 kg increments until the test object fails in one of its elements. This tool has a capacity of up to 100 tons.

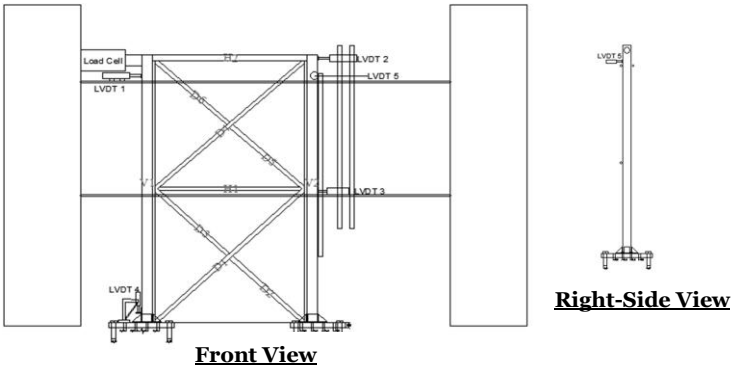

Figure 2. Plane frame loading testing

2.4. Data Analysis Stages

At this stage, the parameters used to determine structural capacity data include deflection. By examining different types of test objects, the effect of varying horizontal bar spacing on the capacity of the plane frame structure can be evaluated. Ductility is calculated by dividing the ultimate deflection value by the deflection value at yield.

During the pushover test, the plane truss specimen was subjected to a static horizontal load until structural failure occurred, recording the maximum load. Measurements of displacement, load, and time data were taken using Linear Variable Differential Transformer (LVDT), strain gauges, and load cells during the test. The load was applied horizontally using a hydraulic jack in increments until reaching the maximum load that caused structural failure in the truss.

The data obtained from the field tests will be compared with the modeling results previously generated using the ETABS application. This comparison allows for the analysis of discrepancies between the experimental and modeled results. The data is then analyzed to determine the reduction factor, which can serve as a reference for similar building construction projects in the future.

The assumptions used in the ETABS modeling include that the material is considered homogeneous and isotropic, and connections are assumed to be perfect without plastic deformation. The analysis was conducted using the Load and Resistance Factor Design (LRFD) approach, assuming the structure's response remains within the elastic deformation range. Additionally, loads were applied monotonically and did not consider dynamic or cyclic effects.

3. Result and Discussion

3.1. Test Results of Physical Properties of Sand (Sieve Analysis)

The examination of the physical properties of sand in this study provides complementary data for planning mortar mixes. Additionally, it ensures that the aggregate used meets the requirements as a mortar-forming material. The results of the sieve analysis of the sand are presented in Table 5.

Table 5. Sieve Analysis Result

Aggregate Type (Kg/l)	Volume Weight (Kg/l)	Specific gravity		Absorption (%)	Fineness Modulus
		SSD	OD		
Fine Sand	2.520	2.768	2.726	1.553	3.730

3.2. Mortar Compressive Strength Testing Results

In this study, three 50 mm test specimens were made for each frame test specimen to control the strength of each test specimen. Mortar Compressive Strength Testing is carried out starting at 14 days of age, aiming to reach K-400 quality. The results of this test provide the compressive strength values of the mortar. The data from the mortar compressive strength testing are shown in Table 6. These results indicate that the compressive strength of the mortar varies among the different types of frames, reflecting the differences in their structural capacities and ductility.

Table 6. Mortar Compressive Strength Testing Results

Test Item Name	Test Item Dimensions			Test Piece Area (cm²)	Load (Kg)	Compressive Strength (Kg/cm²)	Average Compressive Strength (Kg/cm²)
	L (cm)	W (cm)	H (cm)				
RBH Type1	4.97	5.04	5.11	25.05	9,000.00	359.30	408.62
	4.96	4.94	5.25	24.50	9,500.00	387.72	
	4.98	5.20	5.03	25.90	12,400.00	478.84	
RBH Type2	5.04	5.15	5.25	25.96	10,500.00	404.53	415.29
	4.98	5.10	5.22	25.40	12,000.00	472.48	
	4.90	5.09	5.26	24.94	9,200.00	368.87	
RBH Type3	4.98	5.24	4.99	26.10	11,500.00	440.69	420.56
	5.08	5.01	4.98	25.45	11,000.00	432.21	
	4.89	5.26	4.99	25.72	10,000.00	388.78	

3.3. Monotonic Loading Testing (Push Over) Results

The plane frame loading Testing in this study aims to determine the capacity and ductility values of the plane frame. The final results of this test are presented in the form of load-deflection graphs based on the values recorded by LVDT 2. The graphs illustrate the relationship between the applied load and the resulting deflection for each type of plane frame.

Figures 3 show the load-deflection curves for RBH Type 1, RBH Type 2, and RBH Type 3, respectively. These graphs highlight the differences in performance due to varying horizontal bar spacings.

The load-deflection curves indicate the following: RBH Type 1: shows a moderate load capacity and deflection before failure, indicating balanced capacity and ductility; RBH Type 2: exhibits higher deflection at lower loads, suggesting lower capacity but greater ductility compared to Type 1; RBH Type 3: demonstrates the highest load capacity with the least deflection before failure, reflecting greater stiffness and reduced ductility compared to Types 1 and 2.

By comparing these curves, we can evaluate the effect of different horizontal bar spacings on the structural performance of the plane frames. This analysis helps determine the optimal design configuration for maximizing capacity and ductility, providing valuable insights for future construction projects.

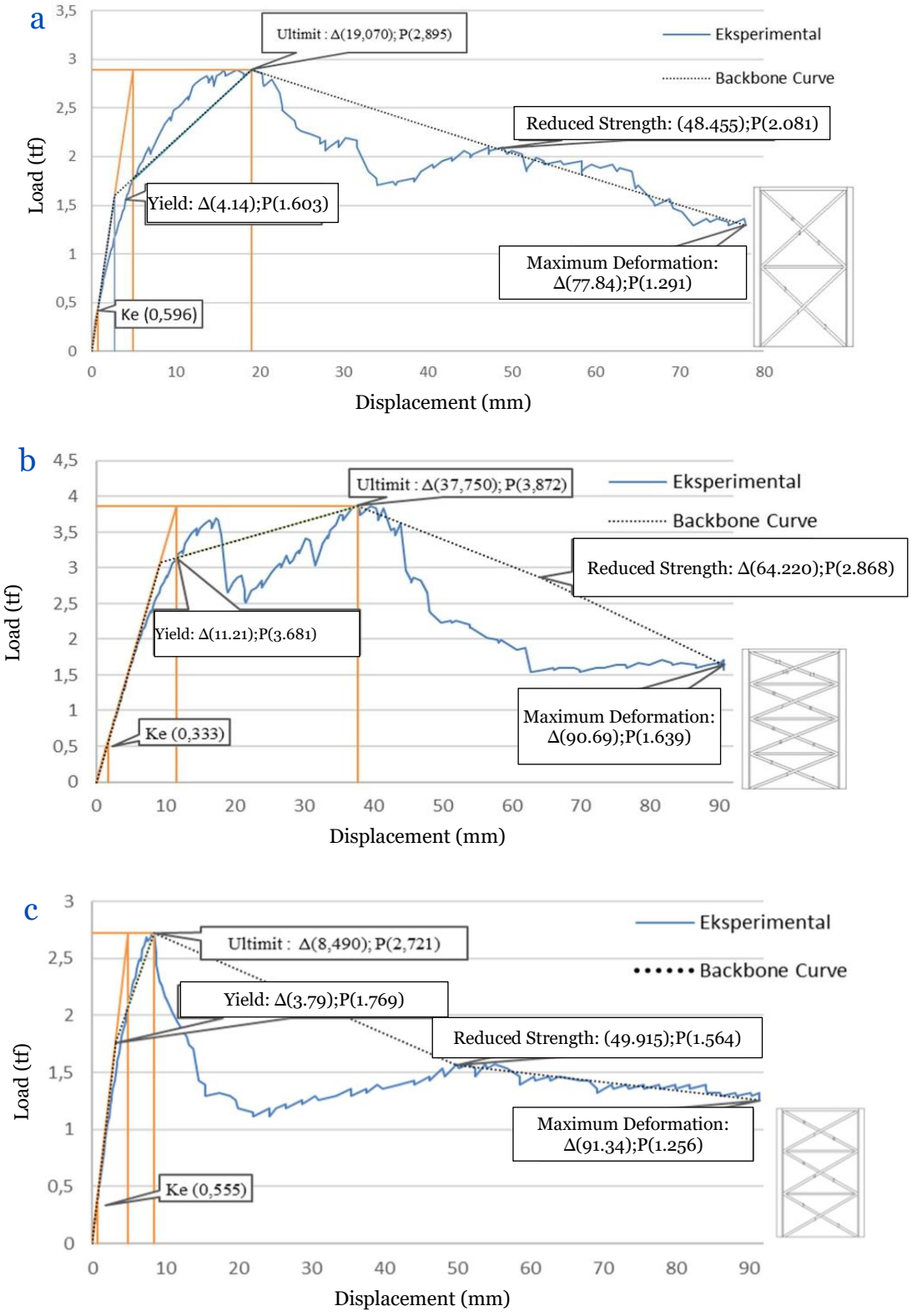

Figure 3. Load-deflection curves for RBH type 1 (a), RBH type (b), and RBH type 3 (c).

From the three graphs of laboratory test results based on the backbone curve analysis above, it can be seen that RBH Type 3 can withstand the greatest maximum capacity with a load of 3.872 tf and a deflection of 37.750 mm. The stiffness value, yield point, ultimate point, reduced strength, and maximum deformation of each type of test object are summarized in Table 7.

Table 7. Backbone Point

Test Item Name	Initial Stiffness (tf/mm)	Backbone Point				Reduced Strength		Maximum Deformation	
		Yield		Ultimite					
		Δ (mm)	P (tf)	Δ (mm)	P (tf)	Δ (mm)	P (tf)	Δ (mm)	P (tf)
RBH Type1	0.596	4.140	1.603	19.070	2.895	48.455	2.081	77.84	1.291
RBH Type2	0.555	3.790	1.769	8.490	2.721	49.915	1.564	91.34	1.256
RBH Type3	0.333	11.210	3.081	37.750	3.872	64.220	1.562	90.69	1.639

From the modeling results in the ETABS application, the RBH Type 1 test object has a maximum capacity of 4.8 tf, RBH Type 2 has a maximum capacity of 5.6 tf, and RBH Type 3 has a maximum capacity of 5.8 tf. These results indicate that there is a discrepancy between the laboratory tests and the ETABS modeling. The experimental values of maximum capacity are lower than the modeled values, suggesting that real-world conditions introduce factors that reduce the structural performance of the plane frames. These differences highlight the need for a reduction factor when applying ETABS modeling results to practical construction projects. From the modeling results in the ETABS application, the RBH Type1 test object has a maximum capacity of 4.8tf, RBH Type2 of 5.6tf, and RBH Type3 of 5.8tf.

3.4. Effect of Horizontal Rods on Plane Truss Capacity

From the load-deflection graph against LVDT 2 (Figure 4), it can be observed that the control plane truss has a very low capacity due to its non-rigid structure [4]. The maximum capacity is only 0.279 tf, even though the deflection has reached 10 cm [7]. The use of variations in the plane truss with horizontal spacing increases the capacity of the plane truss [15]. Specifically, the plane truss with the most horizontal bars has the largest maximum capacity [14]. This increase in capacity is attributed to the addition of horizontal bars, which makes the plane truss more rigid [16]. RBH Type 2 experienced a decrease in capacity compared to RBH Type 1, due to the failure of one of the compressive bars, which caused the plane truss to lose its rigidity [1]. The maximum capacities recorded are as follows: RBH Type 1: 2.895 tf; RBH Type 2: 2.721 tf; and RBH Type 3: 3.872 tf [17].

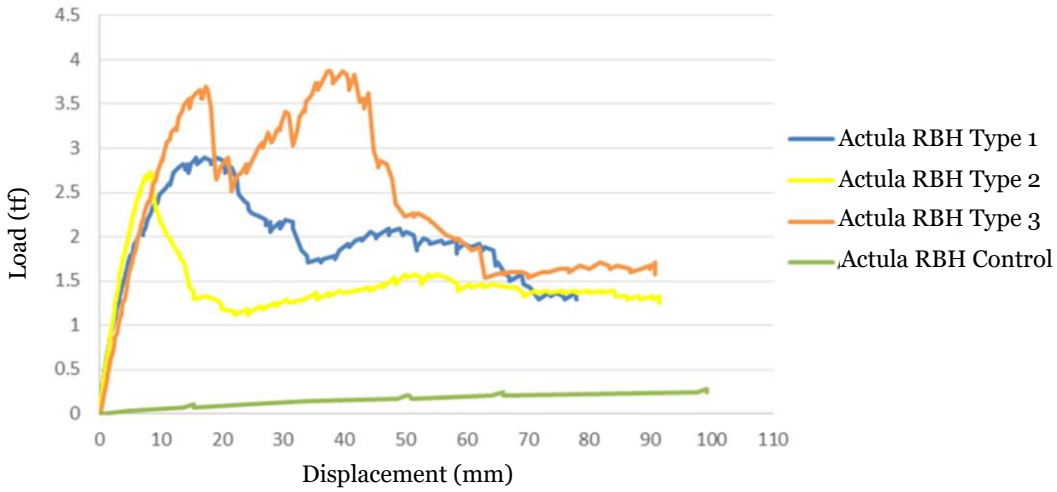

Figure 4. Load-deflection graph of test specimens

The decrease in capacity for RBH Type 2 is attributed to the quality of the connections not meeting expectations, resulting in a reduction in truss rigidity. When comparing RBH Type 1 and RBH Type 2, it can be seen that RBH Type 2 has a decreased capacity of -6.010%. In contrast, RBH Type 3 shows a significant increase in capacity of 33.748% compared to RBH Type 1. Based on the results of structural analysis calculations using the ETABS application, the addition of horizontal bars can increase the plane frame's ability to withstand monotonic loads (pushover). However, the results of laboratory testing show a decrease in capacity for RBH Type 2 by 6.010%. This decrease is

Journal of Sustainable Engineering Insights (JSCEI)

likely due to the quality of the connections not meeting expectations. The percentage increase in the capacity of the plane frame can be seen in Table 8. These results indicate that adding horizontal bars can significantly enhance the load-bearing capacity of the plane truss [10]. However, the quality of construction, especially the connections, plays a critical role in achieving the expected performance [18].

Table 8. Percentage Increase in Capacity

Test Item	Maximum Load (tf)	Deflection at Load Maximum (mm)	Percentage Increase Ability to Wisthand Load Against RBH Type I (%)
RBH Type1	2.895	19.070	-
RBH Type2	2.721	8.490	-6.010
RBH Type3	3.872	37.750	33.748

3.5. Ductility of plane frame

From the results of the load testing of the frame in the laboratory, a graph of the relationship between stress and strain is obtained [19]. This graph is used to determine the ductility value by comparing the deflection at ultimate (Δu) with the deflection at yield (Δy) [20]. Table 9 presents the ductility values for each type of frame based on the laboratory test results. As observed, RBH Type 1 has a ductility of 4.61; RBH Type 2 has a ductility of 2.24; and RBH Type 3 has a ductility of 3.37. These results indicate that RBH Type 1 demonstrates the highest ductility, followed by RBH Type 3, and finally RBH Type 2. This suggests that the design of RBH Type 1 provides the best combination of strength and flexibility among the three types tested. The reduced ductility in RBH Type 2 could be due to premature failure in one of its components, highlighting the importance of quality construction and proper reinforcement to achieve the desired structural performance.

Table 9. Ductility Values of Plane Frame

Test Item	Δ_y (mm)	Δ_u (mm)	$\mu = \Delta u/\Delta_y$
RBH Type1	4.14	19.07	4.61
RBH Type2	3.79	8.49	2.24
RBH Type3	11.21	37.75	3.37

Based on the results obtained, there is a noticeable decrease in the ductility of RBH Type 1, RBH Type 2, and RBH Type 3. This decrease is attributed to the increase in the number of horizontal bars, which contribute to the increased stiffness of the plane frame [21]. Consequently, this increase in stiffness leads to a decrease in ductility [14].

RBH Type 1: despite having the highest ductility value among the three, the introduction of more horizontal bars has slightly reduced its ductility compared to a potentially less stiff configuration. RBH Type 2: shows a significant reduction in ductility, likely due to the structural failure of one of its compressive bars, which compromises the frame's ability to deform plastically. RBH Type 3: although it has a higher ductility than Type 2, it still experiences a reduction in ductility due to the increased stiffness from additional horizontal bars.

The relationship between stiffness and ductility in structural elements is critical. While increasing the number of horizontal bars enhances the overall load-bearing capacity and stiffness of the frame, it also limits the frame's ability to undergo significant plastic deformation before failure, thus reducing its ductility [7]. This trade-off must be carefully considered in structural design to ensure the desired balance between strength and flexibility [17]. In conclusion, the decrease in ductility with the increase in horizontal bars is an important consideration for future design and construction practices, aiming to optimize both the stiffness and ductility of plane frames.

3.5.1 Comparison of plane frame capacity values from ETABS modeling calculations and laboratory test results

From Figures 5, it can be seen that the modeling results in ETABS do not show the yield point. As a result, the ETABS modeling cannot determine the ductility value. This is because the modeling using the ETABS application employs the Load and Resistance Factor Design (LRFD) approach, meaning that the response or performance of the plane frame is assumed to remain within the elastic deformation range.

Journal of Sustainable Engineering Insights (JSCEI)

Theoretical testing using the ETABS application for RBH Type 1, RBH Type 2, and RBH Type 3 yields maximum capacities of 4.8 tf, 5.6 tf, and 5.8 tf, respectively. In contrast, the experimental testing in the laboratory shows maximum capacities for RBH Type 1, RBH Type 2, and RBH Type 3 of 2.895 tf, 2.721 tf, and 3.872 tf, respectively.

The difference in capacity between ETABS modeling and laboratory testing is significant [2]. This discrepancy arises because the analysis using ETABS is conducted within the linear-elastic range, which does not account for the inelastic deformation behavior (including components and joints) that can be critical in real-world scenarios [6].

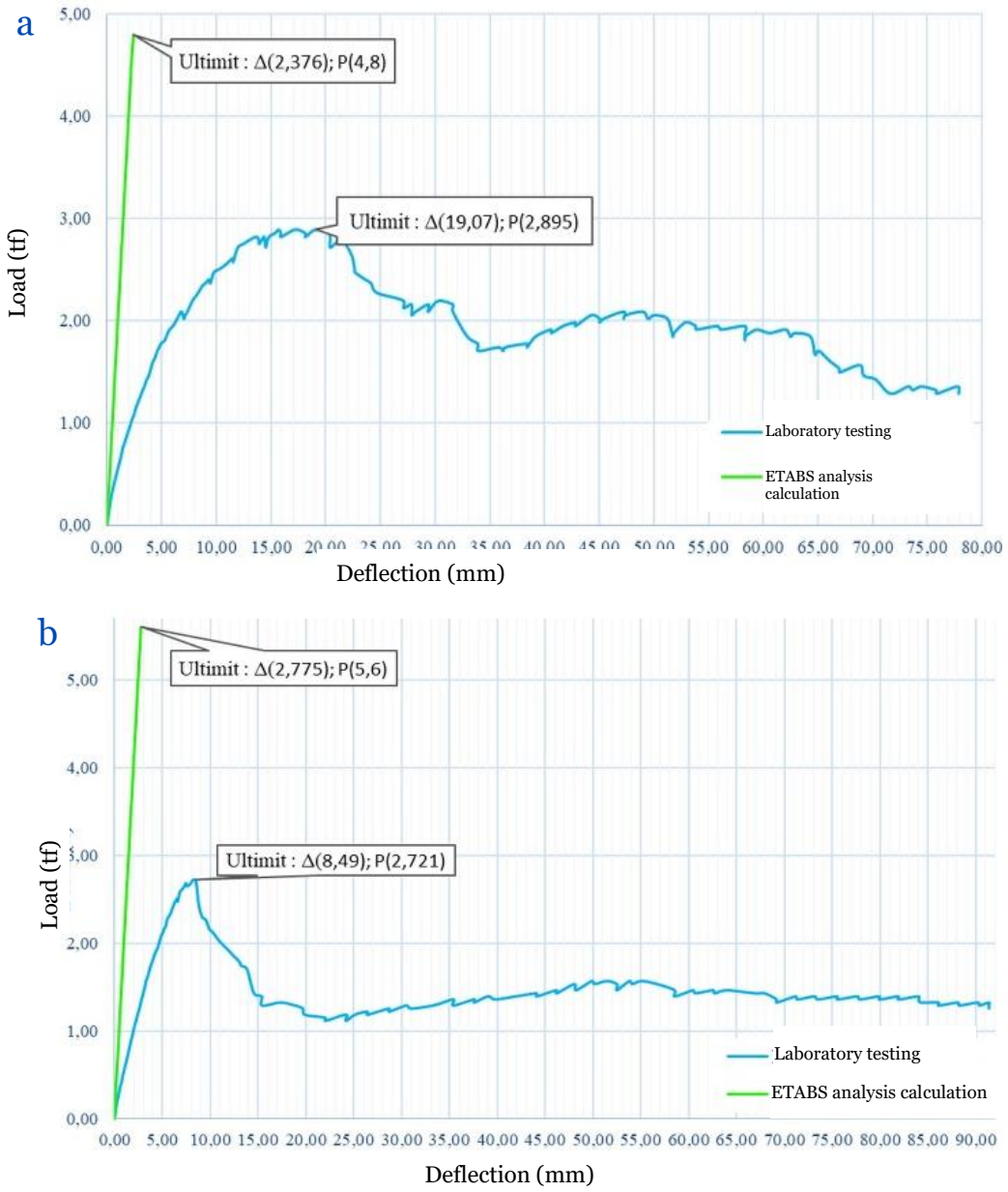

Figure 10. Comparison of laboratory and ETABS results for RBH type 1 (a), RBH type 2 (b), and RBH type 3 (c).

Journal of Sustainable Engineering Insights (JSCEI)

c

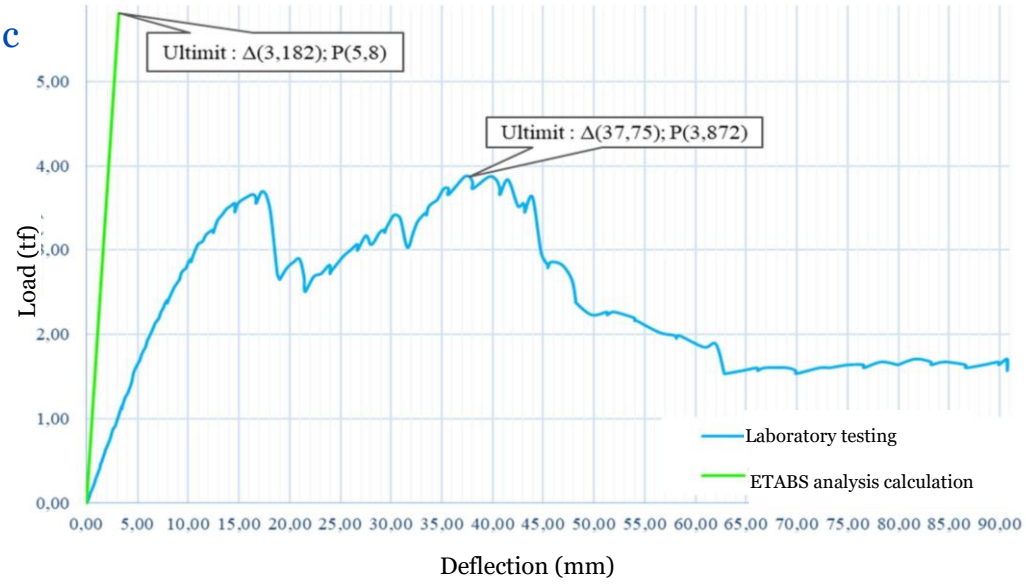

Figure 10. (Continued)

To address this disparity, a reduction factor is needed when using ETABS modeling for similar buildings intended to be applied in the field. The ratio of laboratory test results to ETABS analysis can be seen in Table 10.

Table 10. Ratio of Actual Testing Results to ETABS Analysis

Test Item	Load Maximum		Ratio of Actual Testing to ETABS (%)
	ETABS (tf)	Actual (tf)	
RBH Type1	4.80	2.895	0.60
RBH Type2	5.60	2.721	0.49
RBH Type3	5.80	3.872	0.67

3.5.2 Plane truss failure mode

RBH Type 1: in this test item, when given a load up to 75mm deflection, the first destruction occurred on rod D1 (tensile); on this rod, the expected connection was unable to withstand the tensile force, so it broke at the connection. As a result of the break in the D1 rod, the D3 (compressive), D4 (tensile), and H1 (tensile) rods also failed because there was no longer anything binding at the bottom.

RBH Type 2: in this test item, when given a load up to 75mm deflection, the first destruction occurs in the H1 rod (press); this causes the capacity of the RBH Type 2 plane frame to be no greater than RBH Type 1 because the stiffness of the plane frame is reduced. After the failure of the connection at rod H1, this makes the truss elastic so that the connections at rods D1 (tensile), D3 (compressive), D4 (tensile), D6 (compressive), D7 (tensile), and H2 (tensile) also fail at the connection.

RBH Type 3: in this test item, when loaded up to 75 mm deflection, the first failure occurred in rod H2 (compressive). As a result of the failure of rod H2, rods D6 (compressive) and D8 (compressive) also failed, followed by the failure of rod D2 (compressive).

4. Conclusion

Several conclusions can be drawn from this research:

1) The maximum loads that can be carried by Test Items RBH Type 1, RBH Type 2, and RBH Type 3 are 2.895 tf, 2.721 tf, and 3.872 tf, respectively.
2) The data indicates that the greater the number of horizontal bars used in the plane frame, the higher the load capacity, although a poor connection in RBH Type 2 resulted in a lower load capacity than RBH Type 3.

3) The ETABS analysis shows maximum loads of 4.8 tf, 5.6 tf, and 5.8 tf for RBH Types 1, 2, and 3, respectively, demonstrating that additional horizontal bars increase load capacity in the analysis.
4) The ductility values from laboratory tests are 4.61 for RBH Type 1, 2.24 for RBH Type 2, and 3.37 for RBH Type 3, with the decrease in ductility attributed to increased stiffness from additional horizontal bars.
5) The load-bearing capacity from laboratory tests is smaller than the structural analysis results due to the assumption of perfect rigidity in the analysis, which is not achievable in practical conditions.
6) The comparison ratios of laboratory test results to ETABS analysis for RBH Types 1, 2, and 3 are 0.603, 0.486, and 0.668, respectively.
7) For future research, it is recommended to conduct further studies on non-linear elastic modeling using experimental test information, perform additional experimental testing on structural components to define plastic joints for modeling, and investigate the use of precast concrete as a wall filler.

Acknowledgements:

We would like to express our sincere gratitude for the assistance of the technical staff and colleagues at the Construction and Building Materials Laboratory.

Author Contributions:

M. Saumi Rizaldi contributed in conceptualization, methodology, software, formal analysis, investigation, resources, writing—original draft, and writing—review and editing. Saffuan Wan Ahmad contributed in investigation, formal analysis, visualization, and writing—review and editing. Kavitha P.E contributed in investigation and writing—review and editing. Rahimi A. Rahman contributed in software, visualization, and project administration. All authors have read and agreed to the published version of the manuscript.

Declaration of Competing Interest:

The authors declare that they have no known competing financial interests or personal relationships that could have appeared to influence the work reported in this paper.

References

1. Ghaffar, A. “Strength and Ductility of Hollow Steel Frame Filled with Mortar”. J Struc Eng 146, no. 3, pp. 1-10 (2020).
2. Kim, J., Lee, H. Structural Analysis using ETABS. International Journal of Structural Engineering 8, no. 2, pp. 45-58 (2017).
3. Liu, X., Zhang, Y. Welding Techniques for Hollow Steel Sections. Welding Journal 97, no. 4, pp. 120-130 (2018).
4. Marto, A., Azmi, M. Mix Design of Concrete using SNI Standards. Indonesian Journal of Civil Engineering 12, no. 1, pp. 34-45 (2016).
5. Kafi, M. R. Experimental Study on the Behavior of Innovative Hollow Steel Sections under Axial Compression. Journal of Constructional Steel Research 183, no. 106718 (2021).
6. O'Brien, E., Dixon, D. Practical Guide to Concrete Mixing. Concrete International 37, no. 3, pp. 29-35 (2015).
7. ASTM C.125-1995:61. Standard Definition of Terminology Relating to Concrete and Concrete Aggregates. ASTM International.
8. Ramli, M., Tabatabaei, M. Flow Test Procedures for High-performance Mortar. Materials and Structures vol 46, no. 9, pp. 1513-1523 (2013).
9. Stojković, N. Numerical Simulation of T Joints Constructed from Hollow Steel Sections. Applied Sciences 14, no. 8, p. 3152 (2024).
10. ASCE/SEI 7-16. Minimum Design Loads and Associated Criteria for Buildings and Other Structures. The American Society of Civil Engineers.
11. Balai Besar Teknologi Kekuatan Struktur. SNI 07-8389-2017. Instruksi Kerja Cara Uji Tarik Logam (2017).
12. Standar Nasional Indonesia 1729-2020. Spesifikasi Untuk Bangunan Gedung Baja Struktural. Jakarta: Badan Standarisasi Nasional (2020).
13. Building Seismic Safety Council. Fema 274. Nehrp Commentary on The Guidelines for The Seismic Rehabilitation of Buildings. Washington, D.C.: Federal Emergency Management Agency (1997).

14. Badan Standardisasi Nasional. SNI 03-1729-2002 Spesifikasi Untuk Bangunan Gedung Baja Struktural. Jakarta: Badan Standardisasi Nasional (2002).
15. AISC 360-16. AISC360/16 Specification for Structural Steel Buildings. Chicago 612: American Institute of Steel Construction (2016).
16. Alamsyah, S., Putra, R., Huzaim. Pengaruh Faktor Air Semen Terhadap Perilaku Portal Bidang Baja Hollow yang Diisi Mortar. Journal of The Civil Engineering Student 1, no. 2, pp. 1–7 (2019).
17. Diniar, R.A., Ryanto, R. Analisis Perilaku Struktur Gedung 15 Lantai dengan Sistem Pengaku Dinding Geser (Shear Wall) Type C-Shape Terhadap Load. Prosiding SoBAT (2021).
18. Wenda, K., Zuridah, S., & Hastono, B. Pengaruh Variasi Campuran Mortar Terhadap Kuat Tekan. Jurnal Perencanaan dan Rekayasa Sipil 1, no. 1 (2018).
19. Tjerita, K.N. Metode Elemen Hingga Torsi pada Penampang Batang Non-Circular, Jurnal, Universitas Udayana, Bali (2018).
20. Dewobroto, W., Wijaya, R. Perencanaan, Perilaku dan Keunggulan Portal Momen Rangka Batang Khusus (PMRBK) Terhadap Portal Momen Khusus (PMK) pada Bangunan Baja. Seminar dan Pameran HAKI 2015 - “Challenges in the Future” (2015).
21. ACI Committee 211. Standard Practice for Selecting Proportions for Normal, Heavyweight, and Mass Concrete. Ljnl (2002).